

## A MULTIGRID METHOD FOR RECIRCULATING FLOWS

S. SIVALOGANATHAN AND G. J. SHAW

*Oxford University Computing Laboratory, 8–11 Keble Rd, Oxford, U.K.*

### SUMMARY

The use of multigrid methods in complex fluid flow problems is recent and still under development. In this paper we present a multigrid method for the incompressible Navier–Stokes equations. The distinctive features of the method are the use of a pressure-correction method as a smoother and a novel continuity-preserving manner of grid coarsening. The shear-driven cavity problem is used as a test case to demonstrate the efficiency of the method.

KEY WORDS Multigrid method Pressure correction

### INTRODUCTION

The prediction and simulation of complex recirculating fluid flow phenomena is an area of increasing importance in both an industrial and research context.

The convergence rate of solution procedures for the Navier–Stokes equations is in general strongly dependent on the mesh spacing used to discretize the problem, as well as on the Reynolds number. This has resulted in the need to develop new methods for which high mesh refinement does not result in an unacceptable increase in CPU time.

The multigrid method is an iterative procedure which ideally exhibits grid-independent convergence rates (i.e., the method converges at a rate independent of the mesh length of the grid). It has its origins in the work of Fedorenko<sup>1</sup> and Bakhvalov.<sup>2</sup> The potential of the method has been realized and demonstrated in the solution of various elliptic model problems (see Hackbusch<sup>3</sup> and Wesseling<sup>4</sup>). In the field of incompressible fluid dynamics various publications have appeared in the literature. Brandt and Dinar<sup>5</sup> recommend the use of a distributive Gauss–Seidel scheme as a smoother for the Navier–Stokes equations and Fuchs and Zhao<sup>6</sup> have reported extensively on numerical results obtained using this approach. In contrast Vanka<sup>7</sup> uses a symmetric coupled Gauss–Seidel smoother, thus retaining the full coupling between pressure and velocity, and presents results for a range of test problems. Ghia *et al.*<sup>8</sup> use a streamfunction–vorticity formulation and a multigrid method which uses a coupled strongly implicit procedure as a smoother. They obtain results over a range of Reynolds numbers up to 10 000 for the driven cavity problem on very fine meshes. Our numerical results are assessed against their definitive results later in the paper.

This paper describes a FAS cycling algorithm applied to a finite volume discretization on a staggered mesh. An essential requirement in the design of an efficient multigrid method is a good smoothing procedure. Our proposed smoother for the Navier–Stokes equations is the SIMPLE pressure-correction scheme of Patankar and Spalding.<sup>9</sup> This has been successfully used in many industrial codes as an iterative solver and preliminary experiments indicate that it has good smoothing properties.

A novel feature of our approach has been the manner in which grids have been coarsened so as to ensure that, if the continuity equation is satisfied on the finest grid, then the restricted variables will also automatically satisfy continuity on all coarser grids.

The main emphasis of the paper is on the ability to solve the discrete non-linear system of equations efficiently rather than on accuracy at high Reynolds numbers. To this end, stable upwind approximations to convective terms are used. However, caution must be exercised in interpreting numerical results, since artificially high diffusion arises from the use of upwinding. Strikwerda<sup>10</sup> demonstrates that false scaling effects are also present. Given sound solution procedures for such stable approximations, higher-order accuracy may be obtained by means of various defect-correction techniques or by extrapolation of relative truncation errors—see Brandt.<sup>11</sup>

This paper is the first of two dealing with multigrid pressure-correction methods. Its companion, Shaw and Sivaloganathan,<sup>12</sup> gives a theoretical analysis of the SIMPLE pressure-correction algorithm as a smoothing method.

### GOVERNING EQUATIONS AND DISCRETIZATION

The equations expressing conservation of mass and momentum for an ideal incompressible Newtonian fluid are given by

$$\frac{\partial \rho u^2}{\partial x} + \frac{\partial \rho uv}{\partial y} = -\frac{\partial p}{\partial x} + \frac{\partial}{\partial x} \left( 2\mu \frac{\partial u}{\partial x} \right) + \frac{\partial}{\partial y} \left[ \mu \left( \frac{\partial u}{\partial y} + \frac{\partial v}{\partial x} \right) \right], \quad (1)$$

$$\frac{\partial \rho v^2}{\partial y} + \frac{\partial \rho uv}{\partial x} = -\frac{\partial p}{\partial y} + \frac{\partial}{\partial y} \left( 2\mu \frac{\partial v}{\partial y} \right) + \frac{\partial}{\partial x} \left[ \mu \left( \frac{\partial u}{\partial y} + \frac{\partial v}{\partial x} \right) \right], \quad (2)$$

$$\frac{\partial \rho u}{\partial x} + \frac{\partial \rho v}{\partial y} = 0, \quad (3)$$

$(x, y) \in \Omega$ , where  $x, y$  denote the co-ordinate axes and  $u, v$  the components of the velocity in these directions;  $p$  denotes the pressure,  $\mu$  the viscosity and  $\rho$  the density. In the following description of the discretization it is assumed, for clarity of presentation, that  $\rho$  and  $\mu$  are constants. However, the method to be described is applicable to the case  $\rho = \rho(x, y)$ ,  $\mu = \mu(x, y)$ , for which the extension is straightforward.

The discretized equations are formed using a staggered grid with variables located as shown in Figure 1. There are several methods of devising finite difference approximations, but to ensure that the scheme is conservative a finite volume approach is adopted (see Roache<sup>13</sup>). Due to the staggering of the mesh, the three different types of control volume shown in Figure 2 will be

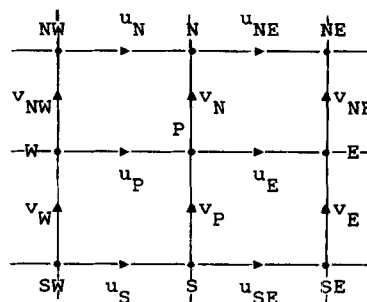


Figure 1. A section of the staggered MAC grid

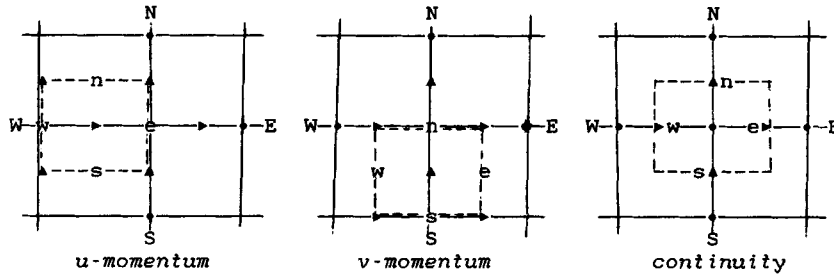


Figure 2. Control volumes for the interior

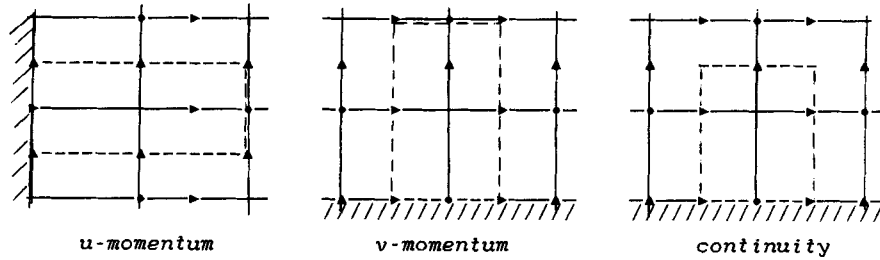


Figure 3. Control volumes adjacent to the boundary

required for the two momentum and continuity equations in the interior, with straightforward modifications near the boundaries as illustrated in Figure 3. The finite volume equations are then derived in a standard manner by integrating (1)–(3) over their respective control volumes, assuming a linear variation between nodes for the dependent variables but constant fluxes over each control volume surface. The source terms are assumed constant over each control volume.

With reference to Figure 1, the resulting discrete equations on a uniform grid  $\Omega_h \subset \Omega$ , of mesh length  $h$ , are

$$\mathbf{L}_h \mathbf{q}_h = \begin{bmatrix} a_h^u & -\mu \delta_h^x \delta_h^y & \delta_h^x \\ -\mu \delta_h^x \delta_h^y & a_h^v & \delta_h^y \\ \delta_h^x & \delta_h^y & 0 \end{bmatrix} \begin{bmatrix} u_h \\ v_h \\ p_h \end{bmatrix} = \begin{bmatrix} 0 \\ 0 \\ 0 \end{bmatrix}, \quad (4)$$

where  $u_h, v_h, p_h$  are gridfunctions defined on  $\Omega_h$  which approximate  $u, v, p$ . The component operators of  $L_h$  are defined by

$$a_h^u \psi(x, y) := a_p^u \psi(x, y) - a_E^u \psi(x + h, y) - a_W^u \psi(x - h, y) - a_N^u \psi(x, y + h) - a_S^u \psi(x, y - h), \quad (5a)$$

$$a_h^v \psi(x, y) := a_p^v \psi(x, y) - a_E^v \psi(x + h, y) - a_W^v \psi(x - h, y) - a_N^v \psi(x, y + h) - a_S^v \psi(x, y - h), \quad (5b)$$

$$\delta_h^x \psi(x, y) := \frac{\psi(x + h/2, y) - \psi(x - h/2, y)}{h}, \quad (6a)$$

$$\delta_h^y \psi(x, y) := \frac{\psi(x, y + h/2) - \psi(x, y - h/2)}{h} \quad (6b)$$

where

$$a_E^u := \frac{1}{h} \max \left( \frac{2\mu}{h}, \frac{1}{2} |(\rho u)_e| \right) - \frac{1}{2h} (\rho u)_e, \quad (7a)$$

$$a_{\text{W}}^u = \frac{1}{h} \max\left(\frac{2\mu}{h}, \frac{1}{2}|(\rho u)_{\text{w}}|\right) + \frac{1}{2h}(\rho u)_{\text{w}}, \quad (7b)$$

$$a_{\text{N}}^u = \frac{1}{h} \max\left(\frac{\mu}{h}, \frac{1}{2}|(\rho v)_{\text{n}}|\right) - \frac{1}{2h}(\rho v)_{\text{n}}, \quad (7c)$$

$$a_{\text{S}}^u = \frac{1}{h} \max\left(\frac{\mu}{h}, \frac{1}{2}|(\rho v)_{\text{s}}|\right) + \frac{1}{2h}(\rho v)_{\text{s}}, \quad (7d)$$

$$a_{\text{P}}^u = \sum_{\alpha} a_{\alpha}^u; \quad (7e)$$

$$a_{\text{E}}^v = \frac{1}{h} \max\left(\frac{\mu}{h}, \frac{1}{2}|(\rho u)_{\text{e}}|\right) - \frac{1}{2h}(\rho u)_{\text{e}}, \quad (8a)$$

$$a_{\text{W}}^v = \frac{1}{h} \max\left(\frac{\mu}{h}, \frac{1}{2}|(\rho u)_{\text{w}}|\right) + \frac{1}{2h}(\rho u)_{\text{w}}, \quad (8b)$$

$$a_{\text{N}}^v = \frac{1}{h} \max\left(\frac{2\mu}{h}, \frac{1}{2}|(\rho v)_{\text{n}}|\right) - \frac{1}{2h}(\rho v)_{\text{n}}, \quad (8c)$$

$$a_{\text{S}}^v = \frac{1}{h} \max\left(\frac{2\mu}{h}, \frac{1}{2}|(\rho v)_{\text{s}}|\right) + \frac{1}{2h}(\rho v)_{\text{s}}, \quad (8d)$$

$$a_{\text{P}}^v = \sum_{\alpha} a_{\alpha}^v; \quad (8e)$$

$\alpha$  ranging over N, S, E, W, points.

The convective mass flux  $(\rho u)_{\text{e}}$  in the  $x$ -momentum equation is an approximation to  $\rho u$  on the eastern wall of the relevant control volume. It is defined as

$$(\rho u)_{\text{e}} = \frac{1}{2}\rho(u_{\text{P}} + u_{\text{E}}).$$

Other mass flux terms are treated analogously.

A more detailed discussion of this discretization can be found in Patankar and Spalding<sup>9</sup> or Sivaloganathan and Shaw,<sup>14</sup> but essentially it simply results in a switching from central to donor cell/upwinding of the convection term plus neglect of diffusion in the direction considered, whenever the appropriate cell Reynolds number is greater than two.

We shall not dwell on the discretization near the boundaries, since the modifications necessary are clear and straightforward.

Any additional scalar conservation law will have nodal values of its dependent variables at the same points as the pressures, and hence a finite control volume identical to the continuity equation control volume can be used to discretize this.

## PRESSURE-CORRECTION METHODS

In this section we describe the SIMPLE algorithm of Patankar and Spalding,<sup>9</sup> setting it in a framework of general pressure-correction methods.

Consider the system

$$\mathbf{L}_h \mathbf{q}_h = \begin{bmatrix} f_h^u \\ f_h^v \\ f_h^p \end{bmatrix}, \quad (9)$$

which is equation (4) with additional source terms which arise during the multigrid process.

Let  $\mathbf{q}_h = (u_h, v_h, p_h)$  be an approximate solution to (9) and  $\hat{\mathbf{q}}_h = (\hat{u}_h, \hat{v}_h, \hat{p}_h) = \mathbf{q}_h + \delta\mathbf{q} = \mathbf{q}_h + (\delta u, \delta v, \delta p)$  be the approximation obtained from  $\mathbf{q}_h$  after a pressure-correction iteration. Substituting  $\hat{\mathbf{q}}_h$  into equation (9) gives

$$(a_h^u u_h - \mu \delta_h^x \delta_h^y v_h + \delta_h^x p_h - f_h^u) + (a_h^u \delta u - \mu \delta_h^x \delta_h^y \delta v + \delta_h^x \delta p) = 0, \quad (10a)$$

$$(a_h^v v_h - \mu \delta_h^x \delta_h^y u_h + \delta_h^y p_h - f_h^v) + (a_h^v \delta v - \mu \delta_h^x \delta_h^y \delta u + \delta_h^y \delta p) = 0, \quad (10b)$$

$$(\delta_h^x u_h + \delta_h^y v_h - f_h^p) + (\delta_h^x \delta u + \delta_h^y \delta v) = 0. \quad (10c)$$

The solution of (10) for  $\delta\mathbf{q}$  yields an exact solution  $\hat{\mathbf{q}}_h$  to (9). However, the system (10) is as difficult to solve as (9) itself. Therefore we attempt to solve a simplified problem. Particular pressure-correction methods, described in the literature, arise from making various assumptions concerning the terms in (10). The first and most common is that the current approximation  $\mathbf{q}_h$  already satisfies the momentum equations of (9). In order to justify this assumption, the pressure-correction method is normally applied only after the approximate independent solution of the momentum equations. In practice this is often interpreted as meaning the application of one or two line relaxation sweeps. Given this assumption, the correction  $\delta\mathbf{q}$  satisfies

$$a_h^u \delta u - \mu \delta_h^x \delta_h^y \delta v + \delta_h^x \delta p = 0, \quad (11a)$$

$$a_h^v \delta v - \mu \delta_h^x \delta_h^y \delta u + \delta_h^y \delta p = 0, \quad (11b)$$

$$(\delta_h^x \delta u + \delta_h^y \delta v) = -(\delta_h^x u_h + \delta_h^y v_h - f_h^p). \quad (11c)$$

The SIMPLE pressure-correction method further neglects the mixed derivative terms and diagonalizes the operators  $a_h^u$  and  $a_h^v$  to give

$$d_h^u \delta u = -\delta_h^x \delta p,$$

$$d_h^v \delta v = -\delta_h^y \delta p,$$

$$(\delta_h^x \delta u + \delta_h^y \delta v) = -(\delta_h^x u_h + \delta_h^y v_h - f_h^p),$$

where  $d_h^u \psi(x, y) = a_h^u \psi(x, y)$  and  $d_h^v \psi(x, y) = a_h^v \psi(x, y)$ .

Hence the corrections  $\delta q$  satisfy

$$\delta u = -(d_h^u)^{-1} \delta_h^x \delta p, \quad (12a)$$

$$\delta v = -(d_h^v)^{-1} \delta_h^y \delta p, \quad (12b)$$

$$[\delta_h^x (d_h^u)^{-1} \delta_h^x + \delta_h^y (d_h^v)^{-1} \delta_h^y] \delta p = \delta_h^x u_h + \delta_h^y v_h - f_h^p. \quad (12c)$$

The algorithm proceeds by applying a few line Gauss-Seidel sweeps to the 'Poisson' equation (12c) for  $\delta p$  and hence obtaining  $\delta u$ ,  $\delta v$  from equations (12a) and (12b). The updated solution  $\hat{\mathbf{q}}_h$  is then defined by

$$\hat{u}_h = u_h + r_{uv} \delta u,$$

$$\hat{v}_h = v_h + r_{uv} \delta v,$$

$$\hat{p}_h = p_h + r_p \delta p,$$

where  $r_{uv}$ ,  $r_p$  are (under) relaxation parameters.

This procedure is applied after a few line relaxation sweeps of the momentum equations, using a relaxation parameter  $r_{\text{mom}}$ . It aims to satisfy the continuity equation assuming that the momentum equations are satisfied.

It is easy to show that the system arising from equation (12c) is singular; and that a unique solution exists (providing the pressure correction  $\delta p$  is fixed at a point) iff the sum of all the right-hand-side terms is equal to zero; otherwise there is no solution. Although this condition is satisfied on the finest grid, for which the source terms are zero, in a multigrid context we have to deal with situations where this may not be true on coarser grids. However, the condition may be enforced on coarser grids by a slight modification of the discretization near the boundary and this is discussed shortly.

### MULTIGRID FOR NON-LINEAR PROBLEMS

The multigrid approach for linear operators is well documented in the literature (see Brandt<sup>15</sup> and Stüben and Trottenberg<sup>16</sup>). For non-linear problems,

$$N_h(\mathbf{q}_h) = f_h, \quad (13)$$

there are two basic approaches. The problem may be globally linearized by Newton's method and the resulting systems solved by linear multigrid. Alternatively, one may use the full method, which improves the approximate solution without global linearization, usually by applying Newton's method only to the local set of unknowns currently being updated. The FAS approach is adopted in this paper.

Denote the application of  $\nu$  non-linear relaxation sweeps to (13) by

$$\bar{\mathbf{q}}_h = S^\nu(\mathbf{q}_h, N_h, f_h).$$

It is imperative that the error in  $\bar{\mathbf{q}}_h$  is smooth in comparison with that of  $\mathbf{q}_h$ . In this connection the SIMPLE algorithm is analysed in Shaw and Sivaloganathan.<sup>12</sup> The following is a brief description of a two-grid FAS method applied to (13).

Smooth an initial approximation  $q_h^i$  by applying  $\nu_1$  iterations of a non-linear smoother  $S$ :  
Assume the existence of a coarse grid  $\Omega_H$ ,  $H > h$ , and grid transfer operators

$$\begin{aligned} R: \mathcal{G}(\Omega_h) &\rightarrow \mathcal{G}(\Omega_H) && \text{(restriction),} \\ P: \mathcal{G}(\Omega_H) &\rightarrow \mathcal{G}(\Omega_h) && \text{(prolongation),} \end{aligned}$$

where  $\mathcal{G}(\Omega_h)$  is the space of gridfunctions defined on  $\Omega_h$ , and similarly for  $\Omega_H$ . The algorithm proceeds as follows (a superscript tilde implies that a gridfunction is unsmooth and a bar that it is smooth):

#### (1) Pre-smoothing

Smooth an initial approximation  $q_h^i$  by applying  $\nu_1$  iterations of a non-linear smoother  $S$ :

$$\bar{q}_h^j = S^{\nu_1}(q_h^i, N_h, f_h).$$

#### (2) Coarse-grid correction

Calculate defect on  $\Omega_h$ :  $\bar{d}_h^j = f_h - N_h(\bar{q}_h^j)$ .

Restrict defect to  $\Omega_H$ :  $\bar{d}_H^j = R\bar{d}_h^j$ .

Restrict  $\bar{q}_h^j$  to  $\Omega_H$ :  $\bar{q}_H^j = R\bar{q}_h^j$ .

Solve

$$N_H(\bar{w}_H^j) = \bar{d}_H^j + N_H(\bar{q}_H^j) \quad (14)$$

for  $\bar{w}_H^j$  on  $\Omega_H$ .

Prolong correction and add to fine grid solution:

$$\bar{q}_h^{j+1} = \bar{q}_h^j + P(\bar{w}_H^j - \bar{q}_H^j).$$

### (3) *Post-smoothing*

The solution is now smoothed to eliminate any high-frequency components introduced by the prolongation:

$$q_h^{j+1} = S^{v_2}(\bar{q}_h^{j+1}, N_h, f_h).$$

A general FAS cycling algorithm is obtained by solving equation (14) itself by a two-grid FAS procedure using a still coarser grid. This idea is applied recursively until we reach a grid coarse enough to permit exact solution.

The particular restriction and prolongation operators are better defined when the method of grid coarsening has been presented in the following section.

## CHOICE OF MULTIGRID COMPONENTS AND SPECIAL FEATURES

In this section we consider some of the special features of our FAS procedure which are particular to the use of pressure-correction methods as smoothers. We present in more detail the strategy adopted for grid coarsening and define the restriction and prolongation operators.

The essential requirement in any multigrid procedure is an efficient smoothing operator. Pressure-correction methods have not been tested in this context, although a number of other non-linear smoothers have been proposed in the literature (see Ghia *et al.*<sup>8</sup> and Brandt and Dinar<sup>5</sup>). In this paper the SIMPLE pressure-correction algorithm is used.

Another point addressed is the existence of a solution to (12c) and the manner of imposing global constraints—in the sense of Brandt,<sup>11</sup> i.e., the fixing of pressure at a point.

It is found that multigrid convergence can be accelerated by a judicious choice of relaxation parameters on each of the hierarchy of grids and this is related to the effective mesh Reynolds number on each grid. At present we follow the general guidelines of Patankar<sup>17,18</sup> in our choice of relaxation parameters on each grid. However, it is hoped that theoretical work currently under progress will help predict optimal relaxation parameters for the grid hierarchy.

### *Grid coarsening*

The motivating factor in our method of grid coarsening has been an attempt to maintain continuity satisfaction between grids. In short, we ensure that each coarse grid continuity control volume is composed of four fine grid continuity control volumes (see Figure 4). Suppose continuity is satisfied on the fine grid. We denote a coarse grid continuity control volume by  $A$  and the four component fine grid control volumes by  $a_i$ ,  $i = 1(1)4$ . Defining the restricted coarse grid velocities to be the mean of their two nearest neighbouring fine grid velocities, it is easy to show that:

$$(\delta_H^x u_H + \delta_H^y v_H)|_A = \sum_{i=1}^4 (\delta_h^x u_h + \delta_h^y v_h)|_{a_i} = 0,$$

$$u_h, v_h \in \mathcal{G}(\Omega_h), \quad u_H, v_H \in \mathcal{G}(\Omega_H).$$

Thus continuity is automatically satisfied on the coarser grid. This manner of grid coarsening has the effect that there are no coincident mesh points on any of the hierarchy of grids. However, it gives rise naturally to compatible momentum control volumes on all grids.

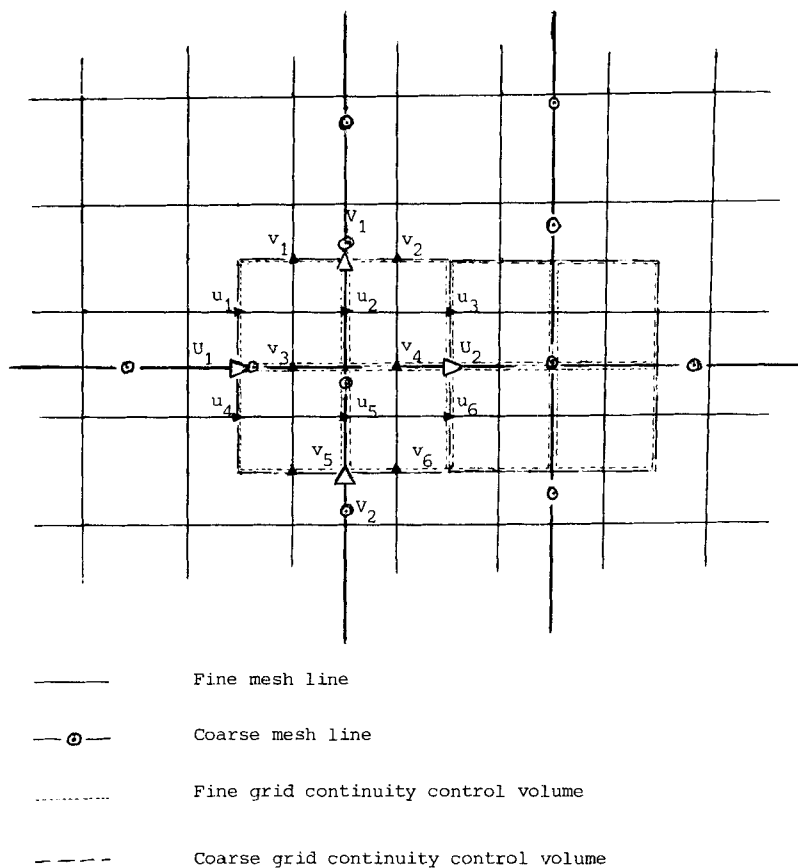


Figure 4. Grid coarsening: ———, fine mesh line; — - - - - , coarse mesh line; - - - - - , fine grid continuity control volume; —————, coarse grid continuity control volume

### Restriction and prolongation

The restriction of velocities is defined as discussed above. Coarse grid pressures  $p_H$  are defined as the mean of the four neighbouring fine grid pressures.

Prolongation operators are derived in all cases using bilinear interpolation.

### Smoothing rate of SIMPLE

Using a two-grid method where the coarse grid problem is solved accurately by performing a large number of SIMPLE iterations, one obtains a prediction of the smoothing capabilities of the SIMPLE algorithm and hence the efficiency of the proposed multigrid method. The two-grid method has been found to be efficient with a smoothing rate ranging from 0.5 to 0.9 for  $Re = 0$  to 10000. Furthermore, the smoothing rate for a given Reynolds number does not deteriorate significantly with grid refinement. Thus the indications are that, if the coarse grid problem—equation (14)—can be solved accurately by the multigrid method, this will give rise to a method that exhibits grid-independent convergence properties over a wide range of Reynolds numbers. A comparison of the practical behaviour with a theoretical analysis of the smoothing rate, using local mode analysis, appears in the companion paper.<sup>12</sup>



*Pressure constraint*

Brandt<sup>11</sup> discusses the treatment of global constraints. For example, since the pressure field in the incompressible Navier–Stokes equations is determined only up to an additive constant, it is necessary to constrain the pressure to determine it uniquely and this can be achieved either by an integral constraint of the form

$$c(x, y) = \iint_{\Omega} p(x, y) dx dy \quad (15)$$

or by a pointwise condition

$$p(x_0, y_0) = 0. \quad (16)$$

According to Brandt, a condition of this nature should not be imposed on the finest grid. Thus, for example, in the case of a discrete non-linear constraint of the form

$$c_h(\mathbf{q}_h) = 0, \quad (17)$$

on a gridfunction  $\mathbf{q}_h$ , the following constraint should be imposed on the coarser grid,

$$c_H(\mathbf{q}_H) = d_H,$$

where

$$d_H = R(-c_h(\mathbf{q}_h)) + c_H(R(\mathbf{q}_h)),$$

and the original constraint (17) should not be imposed on the fine grid. This procedure for the treatment of constraints is completely consistent with the FAS procedure.

In practice, however, imposing the constraint  $p = 0$  at some point  $(x_0, y_0) \in \Omega$  on all grids does not affect the smoothing properties, as it results only in a lowest-frequency error shift. For the test problem considered in this paper—the driven cavity problem—the pressure pointwise condition is enforced at the centre of the cavity by requiring the mean of the four pressure nodes of the mesh cell containing the cavity centre to be equal to zero (due to the manner of grid coarsening, the cavity centre lies in the central mesh cell on all grids).

*Relaxation factors*

In using the pressure-correction algorithm as a smoother, an under-relaxation parameter  $r_{\text{mom}}$  of approximately 0.5 is used in relaxing the momentum equations. Empirically this has been found to be most effective at lower Reynolds numbers and a gradual reduction in  $r_{\text{mom}}$  at higher Reynolds numbers tends to improve the smoothing properties of the algorithm. At the highest Reynolds number solved ( $Re = 10\,000$ ) it has been found that convergence can be accelerated by varying the relaxation parameter on the grids in relation to the mesh Reynolds number (which is related to the amount of artificial viscosity added on each grid). As yet, little theoretical analysis has been carried out, but this is currently under investigation in an attempt to optimize smoothing rates by the correct choice of relaxation factors.

*Existence of solutions to the ‘Poisson’ equation*

The ‘Poisson’ equation for the pressure correction with Neumann conditions is singular, since the matrix has row sum zero. Since the column sum is also zero, there are no solutions unless the right-hand side sums to zero. In this case there is an infinity of solutions. This is related to the compatibility condition for the incompressible Navier–Stokes equations. If the pressure correction

is fixed at one point, there exists a unique solution. This solution will satisfy continuity only if the right-hand side sums to zero. It is possible to zero the sum of the right-hand sides of equation (12c) on all grids in the case where the continuity control volumes are uniform on all grids. This can be achieved by defining the finest grid to have uniform steplength  $h$ , but with steplength  $h/2$  adjacent to the boundary.

### NUMERICAL RESULTS

The driven cavity test problem has been widely used for validating solution procedures for the Navier–Stokes equations and has been the subject of physical flow visualization experiments (see Pan and Acrivos<sup>19</sup> and Koseff and Street<sup>20</sup>).

An isothermal, viscous, incompressible fluid is contained in a square cavity. The problem is to determine the flow induced by the steady, tangential shearing motion of the top wall. Tuann and Olson,<sup>21</sup> in a review paper, discuss most of the important publications on the numerical solution of this problem up to 1978.

Using the non-linear multigrid procedure with the SIMPLE algorithm as a smoother, the test problem has been solved over a range of Reynolds numbers from 1 to 10 000. The results have been compared with the Rolls-Royce industrial code PACE. Early results have been extremely promising. On a typical  $66 \times 66$  mesh the multigrid method is found to be very much faster than the SIMPLE algorithm applied only on the finest grid as an iterative solver.

Tables I and II summarize the convergence characteristics of the multigrid method together with CPU times and also provide a comparison of its performance against PACE. As indicated in Table I, the relaxation parameter has to be reduced with an increase in Reynolds number. Table I gives a strong indication that grid-independent convergence rates are being approached at all Reynolds numbers. It must be noted that for these results the same relaxation parameters have been used over the whole grid hierarchy, with no attempt at optimization on each of the grids. On very coarse grids, as expected, no real advantage is gained in using the multigrid approach;

Table I. Number of multigrid iterations required to reduce residual norm by  $10^{-4}$ . In all cases  $r_{uv} = 1 = r_p$ . Figures in parentheses are CPU times on a DEC Microvax

<i>Re</i>	Finest grid				
	2 6 × 6	3 10 × 10	4 18 × 18	5 34 × 34	6 66 × 66
1 $r_{\text{mom}} = 0.5$	6 (2 s)	7 (7 s)	8 (32 s)	7 (1 min 53 s)	6 (6 min 18 s)
100 $r_{\text{mom}} = 0.35$	11 (3 s)	10 (11 s)	10 (41 s)	13 (3 min 33 s)	16 (17 min 15 s)
400 $r_{\text{mom}} = 0.4$	12 (4 s)	12 (13 s)	14 (56 s)	16 (4 min 14 s)	17 (18 min 5 s)
1000 $r_{\text{mom}} = 0.25$	17 (5 s)	16 (16 s)	19 (1 min 15 s)	22 (5 min 45 s)	24 (25 min)
5000 $r_{\text{mom}} = 0.15$	24 (7 s)	28 (32 s)	34 (2 min 37 s)	35 (11 min 45 s)	35 (36 min 1 s)
10 000 $r_{\text{mom}} = 0.15$	24 (7 s)	27 (31 s)	32 (2 min 28 s)	42 (12 min 49 s)	42 (43 min 14 s)

however, on grid 6 ( $66 \times 66$ ) it is clearly far more efficient to use the non-linear multigrid method as demonstrated by Table II.

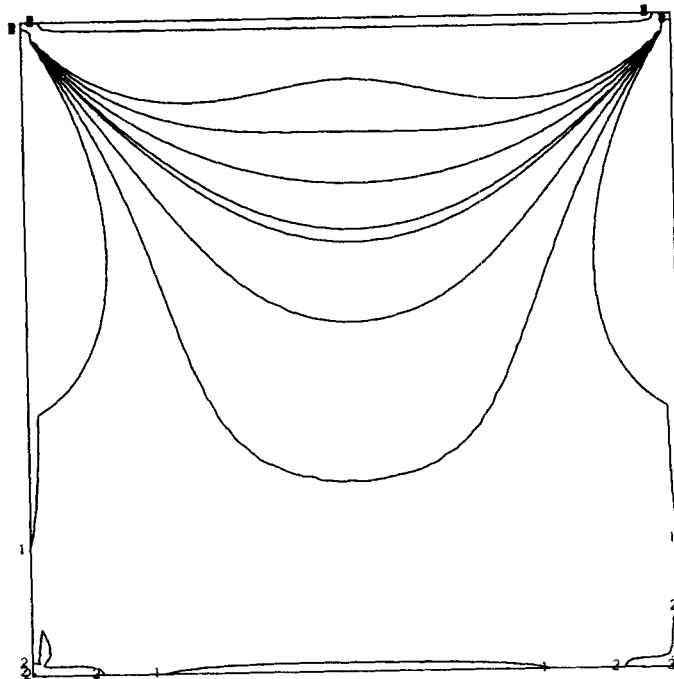
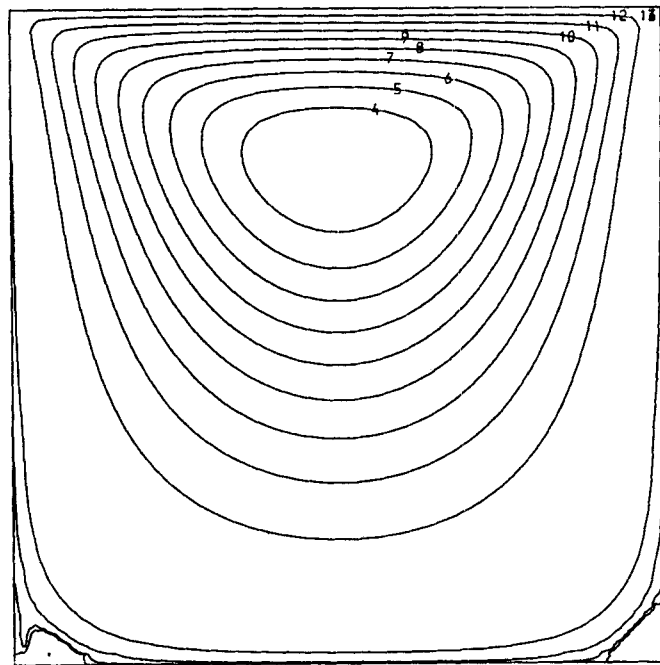
Table III shows the primary and major secondary vortex strengths and location of the vortex centres with variation of the Reynolds number. Up to  $Re = 1000$  the results are in very close agreement with Ghia *et al.*,<sup>8</sup> Gresho *et al.*<sup>22</sup> and Winters and Cliffe.<sup>23</sup> Table IV is a listing of the contour heights for streamfunction, vorticity and pressure plots. Figures 5–8 are plots of streamfunction, vorticity and pressure distributions together with mid-cavity profiles of velocities, streamfunction and vorticity at  $Re = 1$ . The streamfunction is obtained by calculating the vorticity and then solving a Poisson equation by a linear multigrid method. The streamfunction, vorticity and pressure plots are indistinguishable from the results of Winters and Cliffe,<sup>23</sup> who used the ENTWIFE, Harwell finite element package to obtain their results.

Table II. Comparison of multigrid PACE on grid 6 ( $66 \times 66$ ). This table gives residual norm reductions for multigrid and PACE after the same CPU times have elapsed

$Re$	Multi grid	PACE
1	9.60E-05	2.08E-01
100	8.42E-05	1.67E-02
400	8.91E-05	1.59E-02
1000	9.81E-05	4.27E-02
5000	9.17E-05	3.29E-01
10 000	9.85E-05	4.88E-01

Table III. Vortex strength and location

$Re$		Primary	Major secondary
1	$\psi$	-0.100	4.927E-06
	$\omega$	3.217	-2.612E-02
	$\mathbf{x}$	(0.50, 0.77)	(0.05, 0.02)
100	$\psi$	-0.103	1.404E-05
	$\omega$	3.098	-4.131E-02
	$\mathbf{x}$	(0.61, 0.73)	(0.94, 0.06)
400	$\psi$	-0.112	6.627E-04
	$\omega$	2.254	-4.290E-01
	$\mathbf{x}$	(0.56, 0.61)	(0.89, 0.13)
1000	$\psi$	-0.107	1.906E-03
	$\omega$	1.861	-1.201E+00
	$\mathbf{x}$	(0.53, 0.56)	(0.86, 0.11)
5000	$\psi$	-0.068	4.142E-03
	$\omega$	1.001	-3.812E+00
	$\mathbf{x}$	(0.53, 0.53)	(0.89, 0.08)
10000	$\psi$	-0.058	2.929E-03
	$\omega$	0.728	-4.161E+00
	$\mathbf{x}$	(0.55, 0.53)	(0.92, 0.08)

Figure 5.  $\psi$  and  $\omega$  at  $Re = 1$

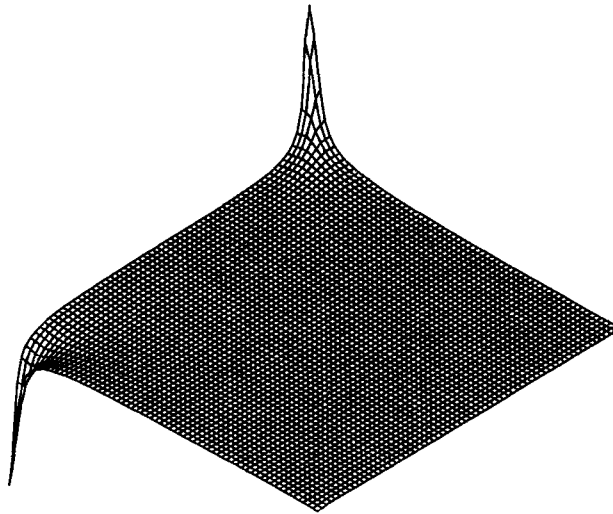
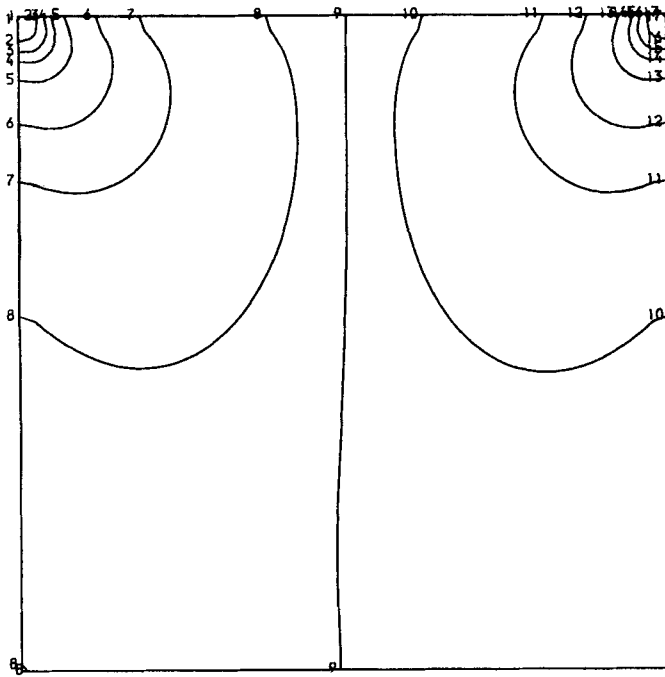
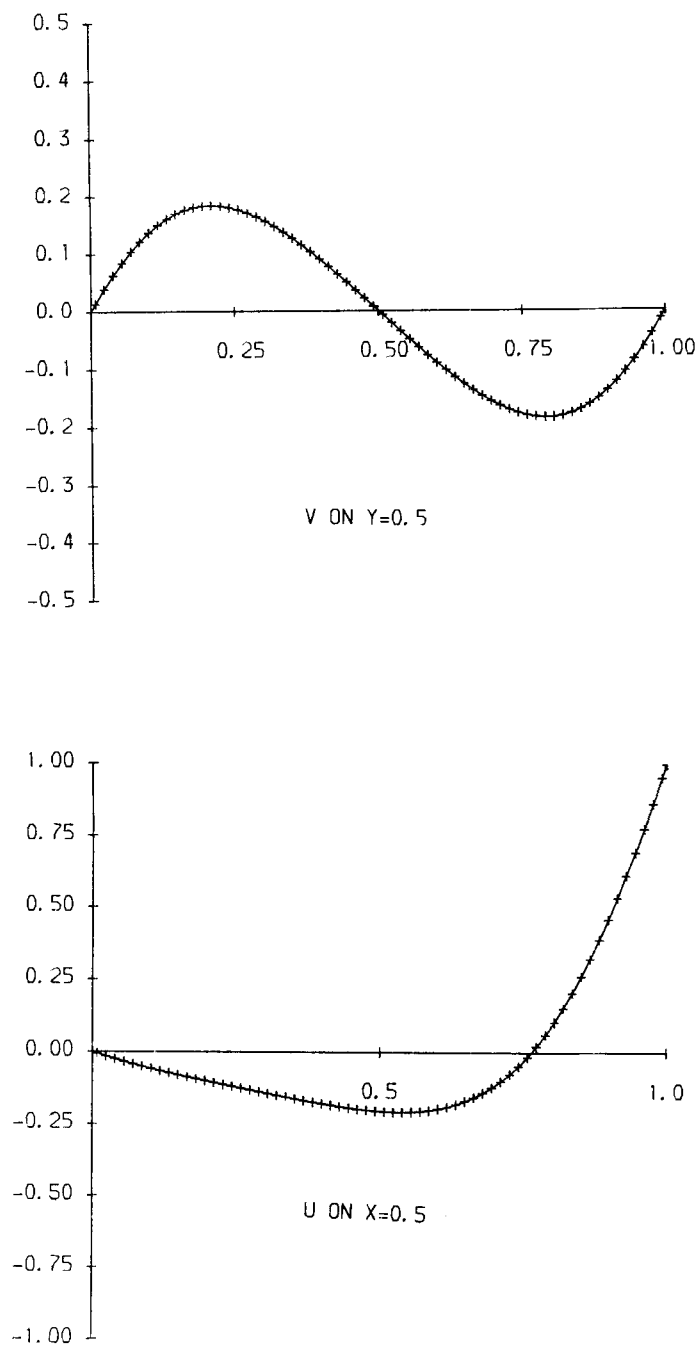


Figure 6. Pressure contours and surface plot at  $Re = 1$

Figure 7. Mid-cavity velocity profiles at  $Re = 1$

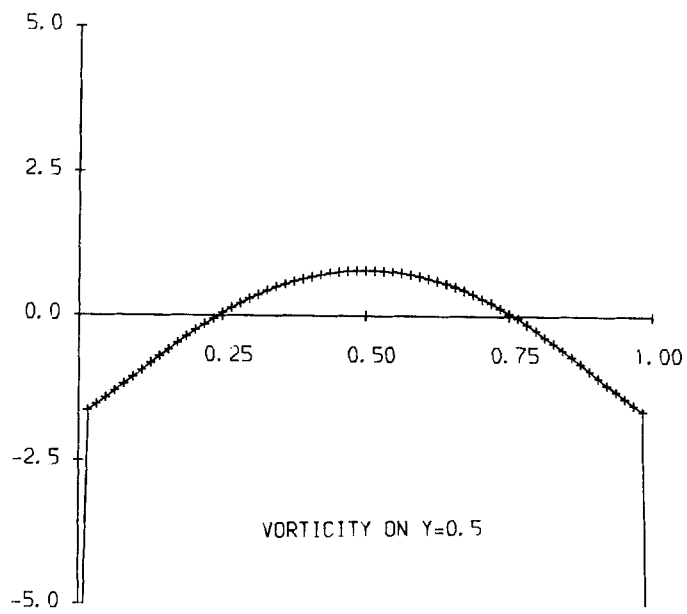
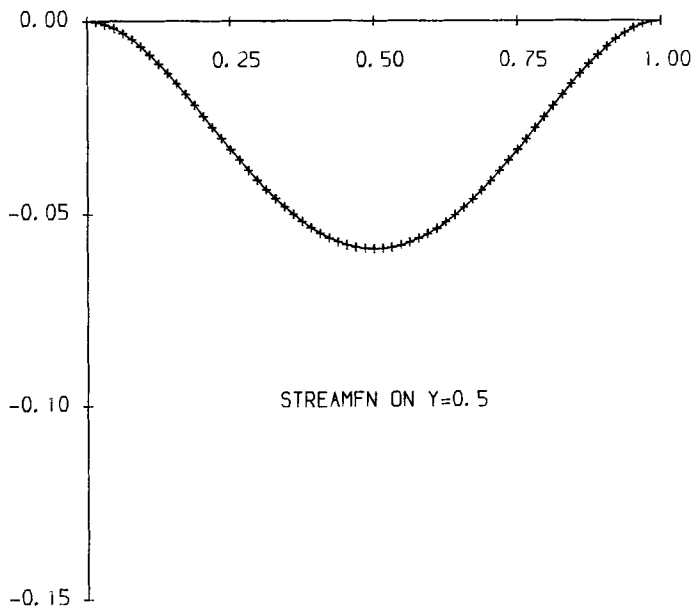


Figure 8.  $\psi$  and  $\omega$  at mid-cavity for  $Re = 1$

Table IV. Contour heights (the contour heights have been chosen so as to facilitate comparison with other published work)

Contour number	$\psi$	$\omega$	$p$
1	-0.12	-1	-180
2	-0.11	0	-60
3	-0.10	1	-40
4	-0.09	2	-30
5	-0.08	2.2	-20
6	-0.07	3	-10
7	-0.06	4	-5
8	-0.05	5	-1
9	-0.04		0
10	-0.03		1
11	-0.02		5
12	-0.01		10
13	-1.E-04		20
14	-1.E-05		30
15	-1.E-06		40
16	0.0		60
17	1.E-04		180
18	5.E-04		
19	1.E-03		
20	5.E-03		

Figures 9–12 are the corresponding results at  $Re = 400$ . These results are in close agreement with Winters and Cliffe.<sup>23</sup> Figure 9 shows the growth in the secondary vortex at the bottom right-hand corner that is expected with an increase in Reynolds number. There is a clear loss of symmetry of the recirculation and the primary vortex centre has moved off the vertical mid-cavity line as shown experimentally (see Pan and Acrivos<sup>19</sup>).

Figures 13–15 are the high-Reynolds-number results (for  $Re = 1000, 5000$  and  $10000$ ). A comparison with Ghia *et al.*<sup>8</sup> shows close agreement for  $Re = 1000$ , with good qualitative agreement for  $Re = 5000$  and  $10000$ . At  $Re = 5000$  the vorticity plot (Figure 14) is closer to that of Ghia *et al.* for  $Re = 1000$ , although the qualitative features of the streamfunction are correct—the tertiary vortex expected only above  $Re = 2500$  is present. It has been found from numerical experiments that the strength of the primary vortex increases with mesh refinement and it is clear that the weak primary vortices shown in Figures 14 and 15 would have been improved by the use of a finer grid. For a particular mesh refinement, an increase in Reynolds number after a certain critical Reynolds number (dependent on the mesh refinement) will result in no additional features being picked up, since the discretization always maintains the mesh Reynolds number below two. In comparing our results with those of Ghia *et al.*,<sup>8</sup> it should be noted that our finest meshes have (at best) mesh spacings double those of the Ghia *et al.* fine grids.

## CONCLUSIONS

An efficient non-linear multigrid method using the SIMPLE pressure-correction scheme has been presented. The numerical results illustrate that it is very much faster than PACE, a code that uses SIMPLE as an iterative solver.



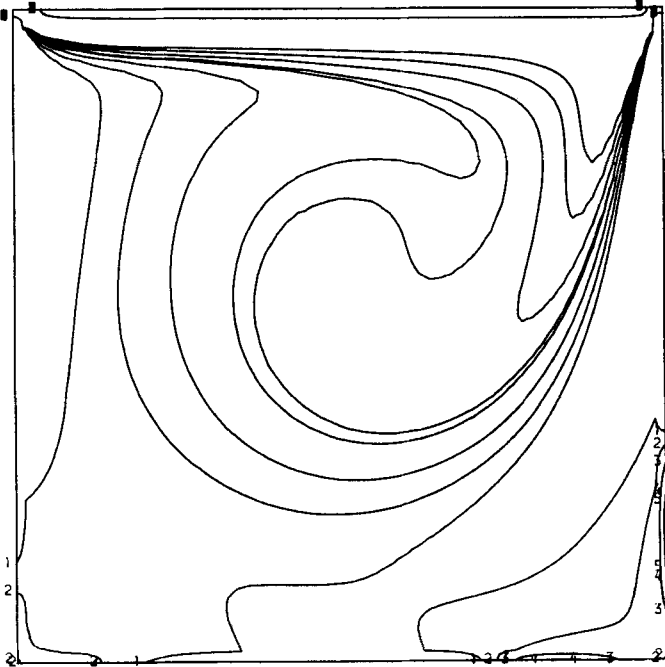
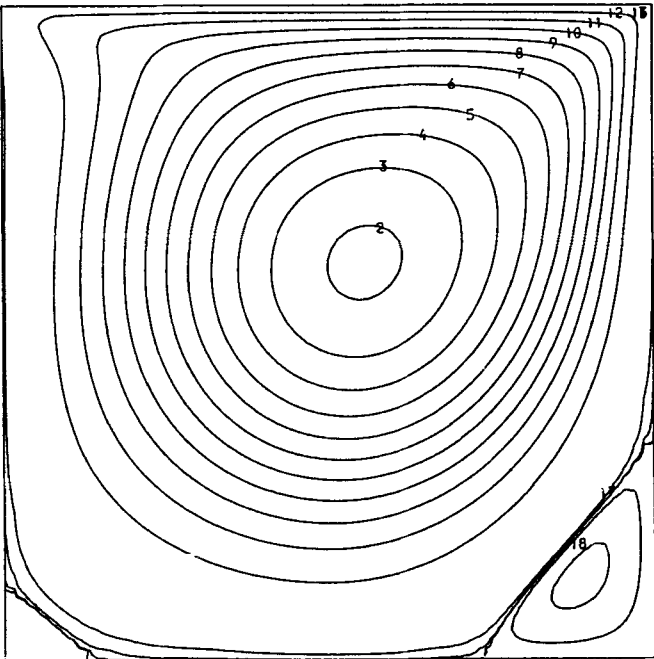


Figure 9.  $\psi$  and  $\omega$  at  $Re = 400$

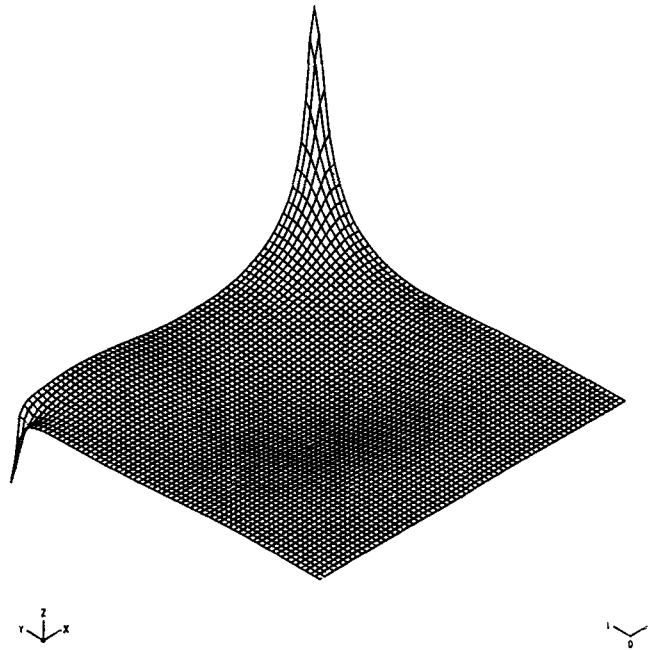
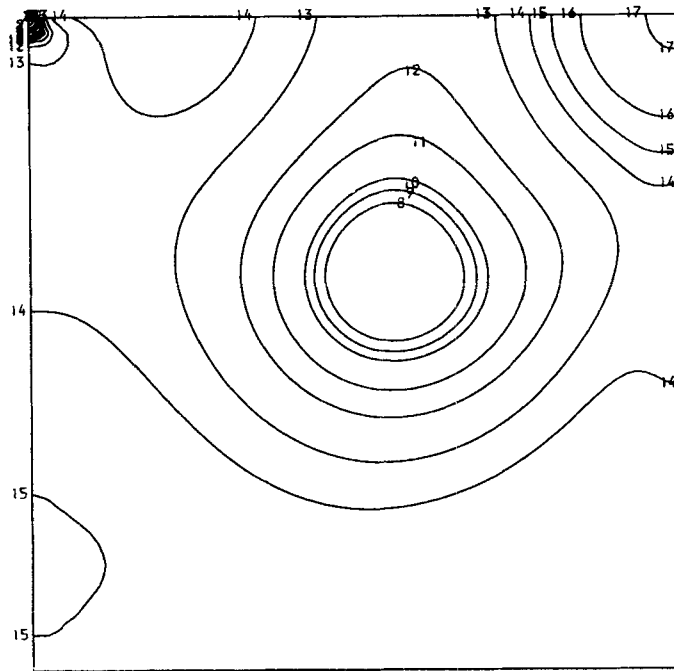


Figure 10. Pressure contours and surface plot at  $Re = 400$

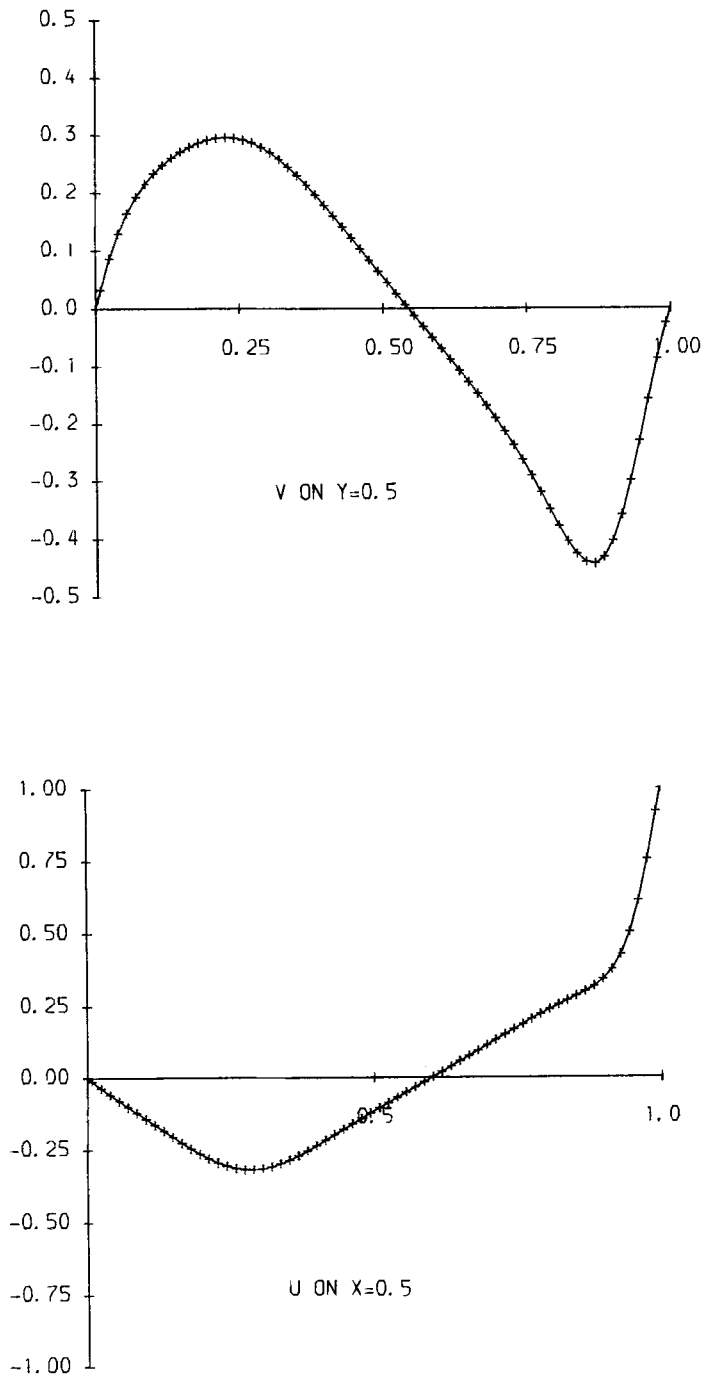
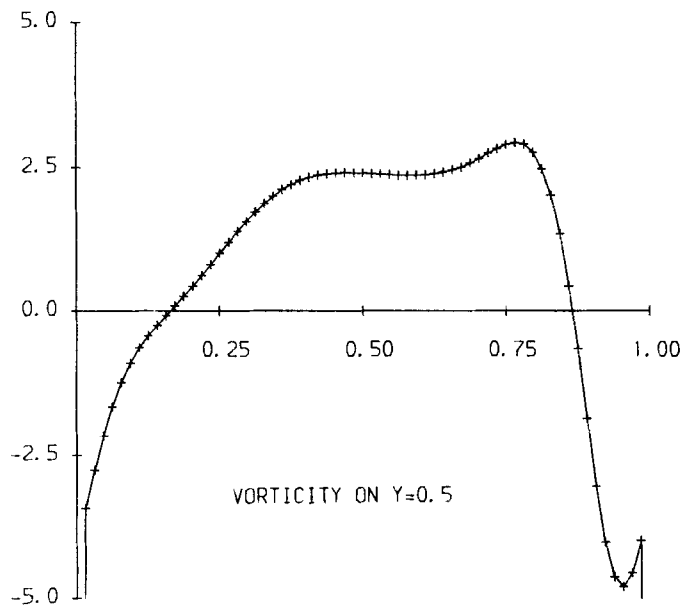
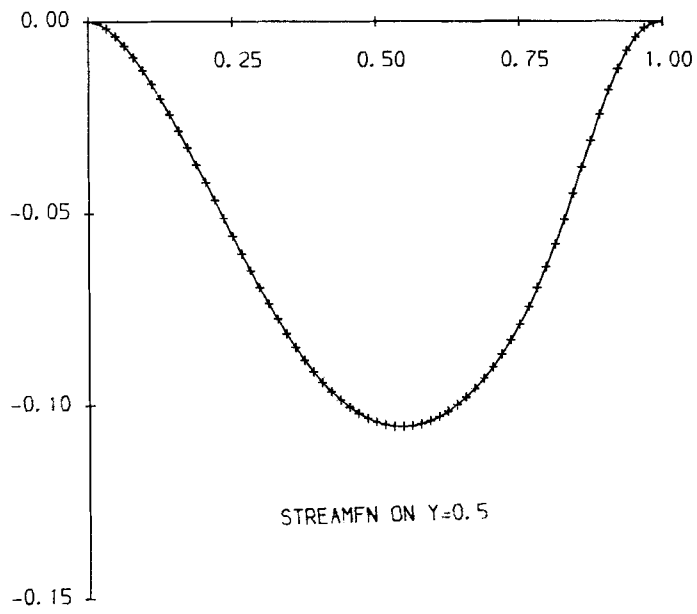


Figure 11. Mid-cavity velocity profiles at  $Re = 400$

Figure 12.  $\psi$  and  $\omega$  at mid-cavity for  $Re = 400$

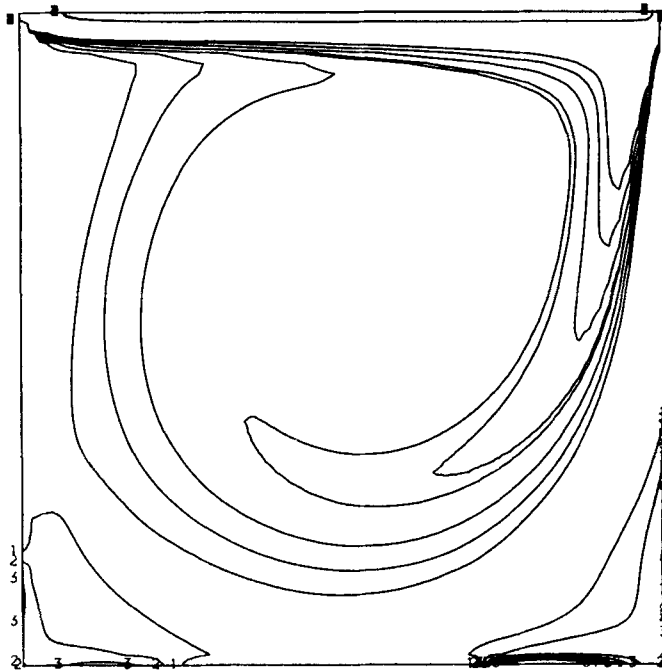
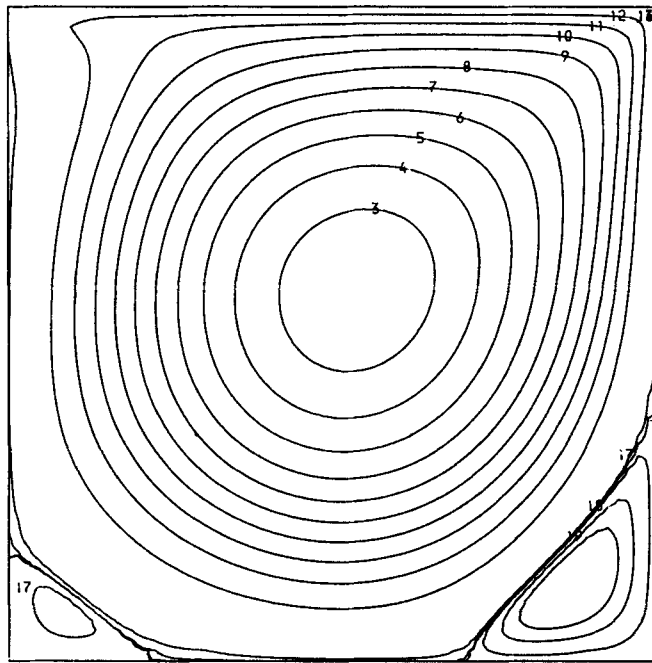
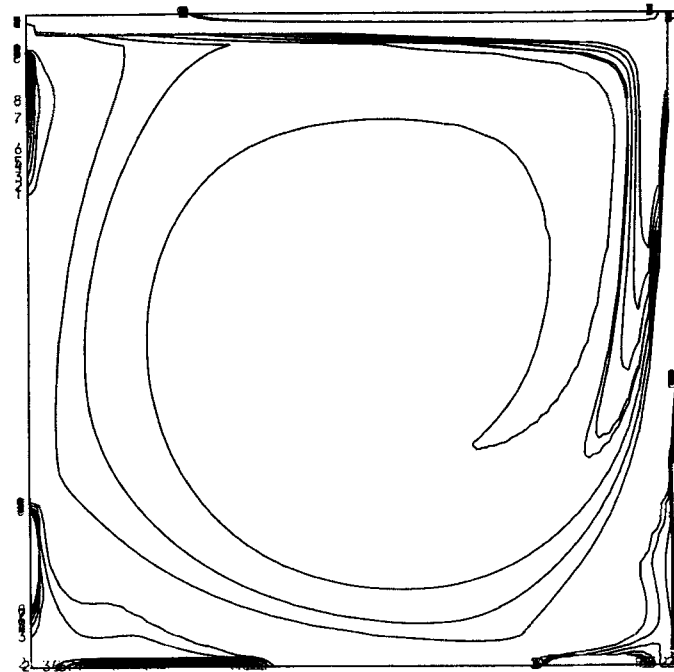
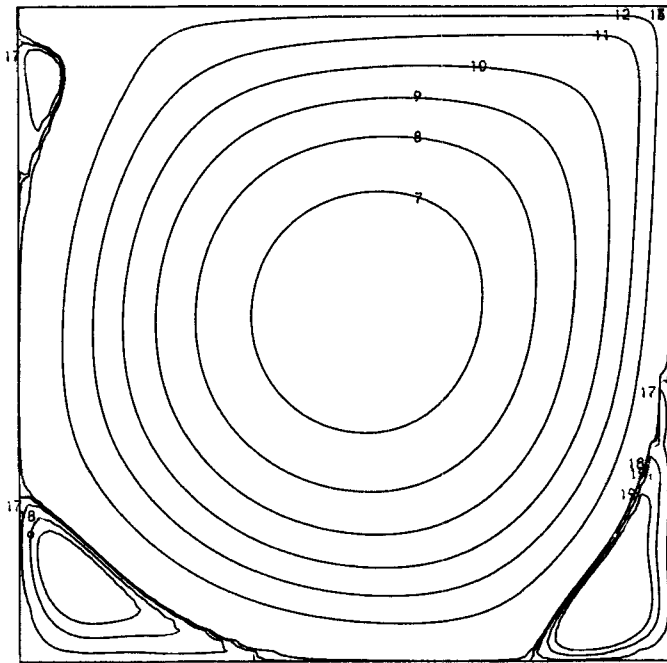


Figure 13.  $\psi$  and  $\omega$  at  $Re = 1000$

Figure 14.  $\psi$  and  $\omega$  at  $Re = 5000$

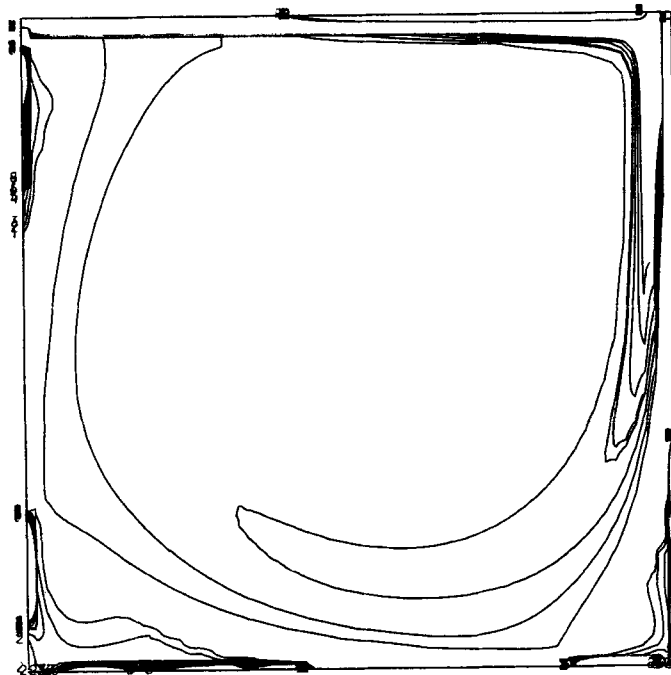
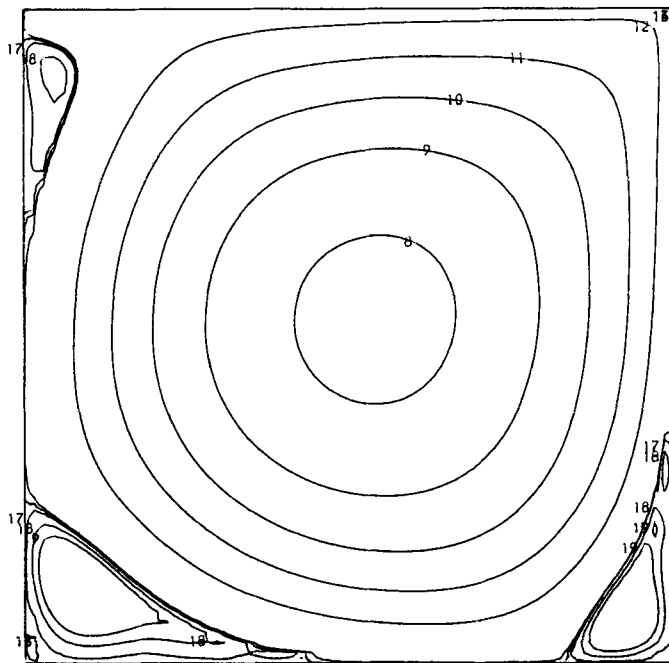


Figure 15.  $\psi$  and  $\omega$  at  $Re = 10000$

The indication is that, if equation (14) can be solved accurately, then grid-independent convergence rates can be obtained at all Reynolds numbers. This has indeed been achieved between the two finest grids and it is likely that further modification to the method could render it still more efficient. The optimization of the relaxation factors on each grid could lead to grid-independent convergence rates even on the coarser grids. It is possible that a local mode analysis would reveal the optimum relaxation parameter (as a function of the mesh Reynolds number) necessary to achieve this.

The aim of the paper—as stated in the Introduction—of developing a sound solution procedure for stable first-order discretizations, has been achieved. This opens the way for the development of fast methods with higher-order accuracy utilizing defect-correction techniques.

#### ACKNOWLEDGEMENTS

The authors would like to thank the SERC and Rolls-Royce for financial support during the course of this research.

#### REFERENCES

1. R. P. Fedorenko, 'A relaxation method for solving elliptic difference equations', *USSR Comput. Math. Math. Phys.*, **1**, 1092–1096 (1962).
2. N. S. Bakhvalov, 'On the convergence of a relaxation method with natural constraints on the elliptic operator', *USSR Comput. Math. Math. Phys.*, **6**, 101–135 (1966).
3. W. Hackbusch, 'On the multi-grid method applied to difference equations', *Computing*, **20**, 291–306 (1978).
4. P. Wesseling, 'A robust and efficient multigrid method', *Lecture Notes in Mathematics*, **960**, Springer-Verlag, New York, 1981, pp. 614–630.
5. A. Brandt and N. Dinar, 'Multigrid solutions to elliptic flow problems', in S. V. Parter (ed.), *Numerical Methods for PDEs*, Academic Press, New York, 1979, pp. 53–147.
6. L. Fuchs and H. S. Zhao, 'Solution of 3-D viscous incompressible flows by a multi-grid method', *Int. j. numer. methods fluids*, **4**, 539–555 (1984).
7. S. P. Vanka, 'Block-implicit multigrid solution of the Navier–Stokes equations in primitive variables', *J. Comput. Phys.*, **65**, 138–158 (1986).
8. U. Ghia, K. N. Ghia and C. T. Shin, 'Solution of the incompressible Navier–Stokes equations by a coupled strongly-implicit multi-grid method', *J. Comput. Phys.*, **48**, 387–411 (1982).
9. S. V. Patankar and D. B. Spalding, 'A calculation procedure for heat and mass transfer in 3-D parabolic flows', *Int. J. Heat Mass Transfer*, **15**, 1787–1806 (1972).
10. J. C. Strikwerda, 'Upwind differencing, false scaling and nonphysical solutions to the driven cavity problem', *J. Comput. Phys.*, **47**, 303–307 (1982).
11. A. Brandt, 'Guide to multigrid development', *Lecture Notes in Mathematics*, **960**, Springer-Verlag, New York, 1981, pp. 220–312.
12. G. J. Shaw and S. Sivaloganathan, 'On the smoothing properties of the SIMPLE pressure-correction algorithm', *Int. j. numer. methods fluids*, **7**, 441–461 (1987).
13. P. J. Roache, *Computational Fluid Dynamics*, Hermosa, Albuquerque, 1982.
14. S. Sivaloganathan and G. J. Shaw, 'A multigrid pressure correction method for incompressible flows', *Oxford University Computing Laboratory Report 86/20*, 1986.
15. A. Brandt, 'A multi-level adaptive solutions of boundary value problems', *Math. Comput.*, **31** (138), 333–390 (1977).
16. K. Stüben and U. Trottenberg, 'Multi-grid methods: fundamental algorithms, model problem analysis and applications', *Lecture Notes in Mathematics*, **960**, Springer-Verlag, New York, 1981, pp. 1–176.
17. S. V. Patankar, 'A calculation procedure for two dimensional elliptic situations', *numer. Heat Transfer*, **4**, 409–425 (1981).
18. S. V. Patankar, *Numerical Heat Transfer and Fluid Flow*, Hemisphere, Washington DC, 1980.
19. F. Pan and A. Acrivos, 'Steady flows in rectangular cavities', *J. Fluid Mech.*, **28**, 643–655 (1967).
20. J. R. Koseff and R. L. Street, 'Visualisation studies of a shear driven three-dimensional recirculating flow', *ASME J. Fluids Eng.*, **106**, 21–29, 385–398 (1984).
21. S. Y. Tuann and M. D. Olson, 'Review of computing methods for recirculating flows', *J. Comput. Phys.*, **29**, 1–19 (1978).
22. P. M. Gresho, S. T. Chan, R. L. Lee and C. D. Upson, 'A modified finite element method for solving the time dependent, incompressible Navier–Stokes equations', *Int. j. numer. methods fluids*, **4**, 619–640 (1984).
23. K. H. Winters and K. A. Cliffe, 'A finite element study of driven, laminar flow in a cavity', *Harwell Report AERE-R9444*, 1979.